FUDMA Journal of Sciences (FJS)
ISSN online: 2616-1370
ISSN print: 2645 - 2944
Vol. 8 No. 1, February, 2024, pp 208 - 216
DOI: https://doi.org/10.33003/fjs-2024-0801-2264

SYNTHESIS AND CHARACTERIZATION OF NOVEL ZEOLITE-X ENCAPSULATED Cu (II) PHTHALOCYANINE COMPLEX FOR SMALL MOLECULE ADSORPTION

[1]Okeniyi, S. O., [1]Omale, P. E., *[2]Shittu, A., [1]Mohammed, Y., [1]Itiveh, G. O.

[1]Department of Chemistry, Nigerian Defence Academy Postgraduate School Kaduna State, Nigeria.
[2]Department of Science Education, School of Technical Education, Yaba College of Technology Yaba Lagos, Nigeria.

*Corresponding authors' email: abdulrazakshittu@yabatech.edu.ng

ABSTRACT

Zeolite Na-X was successfully synthesized from Oke-Ako raw kaolin clay through a series of processes. Raw kaolin was soaked, beneficiated, and calcined to obtain reactive amorphous metakaolin. Dealumination of metakaolin was carried out using tetraoxosulphate (VI) acid, and the resulting gel was aged before crystallization at 110oC for 8 hours. Characterization using XRF, XRD, SEM, FT-IR, and BET revealed positive outcomes in the zeolitization process. The XRF analysis confirmed the success of the pretreatment and zeolitization processes. XRD showed enhanced crystallinity for beneficiated, metakaolin, and zeolite-X at 8 hours of crystallization. SEM images of synthesized zeolite-X at 8 hours displayed desirable characteristics. XRF results indicated Si/Al values of 1.95 and 1.78 for D5ZNa-X and ZNa-X, respectively. Both exhibited sharper zeolitic characteristic O-H stretching bands at 3362 cm−1 and Si-O stretching bands at 969 cm−1. The specific surface area was significantly larger in ZNa-X (266.97 m2/g) compared to D5ZNa-X (105.747 m2/g). This confirms the successful production of zeolite-X from Oke-Ako kaolin, supported by literature comparisons. Overall, these results contribute insights into zeolite behavior as ammonia adsorbents, essential for optimizing ammonia removal applications and environmental remediation solutions.

Keywords: Beneficiation, Metakaolin, Dealumination, X-Ray Flouresence, Brunauer-Emmett-Teller (BET), Crystalization, Zeolitization

INTRODUCTION

Zeolites are an important class of crystalline, micro porous, aluminosilicate materials with a three dimensional fully cross linked open framework structures that form uniformly sized pores of molecular dimensions. (Babalola *et al*., 2017). Zeolite have various industrial applications as adsorbents in separations, ion exchange ability, purification processes, environmental pollution control, molecular sieve and acidic catalysts for size and shape selective catalytic reactions. ((Perez, *et al*., 2022, Ren). There are many types of natural zeolites that have been identified; they are in various forms such as clinoptilolite, mordenite, stilbite, phillipsite, chabazite, and limonite, (Vera-puerto *et al*., 2020). Zeolites are stable solid and can resist high temperatures since they have melting points over 1000°C.The use of cheap and readily available materials such as kaolin to serve as a combined source of silica and alumina is highly desirable. The use of Oke-Ako Nigerian kaolin (OANK) to prepare zeolite-X is for an improved industrial value development. Nowadays, commercial synthetic zeolites are used more frequently than natural zeolites due to their purity of the crystalline products and the uniform particle sizes (He *et al* ., 2021). The main advantages of synthetic zeolites in comparison to natural ones are that they can be engineered with extensive variety of pore sizes and chemical properties and thermally stability. (Noviello *et al*., 2021).In spite of the wide usage of Kaolin for the synthesis of Zeolites no attempt has been made previously to develop Zeolite from Oke-Ako Ijebu-Ode kaolin clay under various operating conditions. In this research work, full characterization of Nigerian Kaolin clay from Oke-Ako Ijebu-Ode deposit was processed

MATERIALS AND METHODS

Sample collection

The starting material tagged (ROA) was geo-referenced from Oke-Ako village in Ijebu–Ode local government area of Ogun State, Nigeria. Sample Codes- (OAK) Oke-Ako Kaolin. - (ZNa-X) Calcinated Zeolite-X. - (D5ZNa-X) Dealuminated five min. Zeolite-X.

Beneficiation of Sample

Exactly 1.5 kg of the Oke-Ako kaolin was soaked with water for a duration of six days, in order to purify it from physically and chemically presence impurities such as soluble salts, grits and metallic oxides of Fe_2O_3, MgO, Na_2O CaO, $CaCO_3$, etc. to Finally the solid cake was split into smaller sizes and open dried in the laboratory for 4 days and further dried at 150°C in an electric oven for 4 hours, after which it was milled and subsequently packaged in a plastic sample container with cover for analysis and calcination, (Ayele, 2018)

Calcination of Sample

In this process, the Beneficiated sample was heated in a programmed Muffle electric furnace from room temperature (T) (31ºC) to the calcinations temperature Tcal of (650ºC) for 3hrs. by evenly placing 500 grams of beneficiated kaolin evenly on a Ceramic crucible to allow for a relative good heat distribution, in order to improve the specific heat capacity and latent heat of kaolin. The metakaolin obtained was then cooled in a desiccator, prior to characterization and usage. (Macivers *et al*., 2020)

Dealumination of Calcined Clay

The prepared metakaolin was then treated using H_2SO_4 in order to get the desired Si/Al values of 1.9 to 2.5 by reducing the alumina contents in the metakaolin. This is because each type of synthetic zeolite depends on the Si/Al value for its synthesis. The dealumination reaction was carried out at a temperature range of between 90-100ºC using the conventional method and at ambient temperature for alternative method using 60% molar H_2SO_4.

Equation 1:
Al_2O_3 (s) + $3H_2SO_4$ (aq) ↔ $Al_2(SO_4)_3$ (aq) + $3H_2O$…. Dealumination.

In this study, the conventional dealumination and the alternative method were used in the dealumination of the metakaolin. The method involved the reaction of the metakaolin with Sulphuric acid (H_2SO_4) and deionized water, with the application of heat from the heating mantle for conventional method and direct reaction of the sulphuric acid with the metakaolin sample at ambient temperature. Samples were added for reaction to commence and proceed for a specified reaction time of 5,10, 15 minutes for both methods respectively. As soon as the reaction time elapsed, the reaction was terminated by adding enough distilled water. The resulting mixture were separated using gravimetric method. Dealuminated metakaolin obtained was continuously washed with distilled water until the absence of sulphate ion was confirmed (Bawa *et al* 2017)

Gel Formation

The Silica/Alumina (SiO_2/Al_2O_3) values used in this work is obtained from the compositional analysis of the dealuminated samples as shown in Table 4.3, The volume of water and the mass of sodium hydroxide required for gelating 30g of dealuminated metakaolin was at a molar concentration dilution of 2.8M for, 26g of Sodium hydroxide pellets in a teflon bottle and mixed with the required quantity of deionized water until the sodium hydroxide pellets were dissolved completely after been thoroughly mixed using a magnetic stirrer, 30g of dealuminated metakaolin sample was then added to the NaOH solution. The content was continuously stirred with magnetic stirrer to achieve homogeneity for 10 minutes. The resulting aluminosilicate gel was put in an autoclave reactor, sealed and left in a static condition to age for 4 days at ambient conditions and crystallized for 8 hrs, (Olaremu *et al.,* 2018). The reaction mixtures was washed and filtered with deionized water until the pH of the filtrate is neutral to pH meter, finally the samples were dried overnight at 100^0C before material characterization. (Ayele *et al.,* 2018).

Equation 2:
$6Al_2Si_2O_7 + 12NaOH \rightarrow Na_{12}(AlO_2)_{12}(SiO_2)_{12} + 6H_2O$
(metakaolinite) (zeolite-X gel formation)

Gel Aging

Gel aging can be considered as, an interval composition reaction of the gel and the crystallization process. In this synthesis, the gel was kept undisturbed (aged) at ambient temperature. To study the effect of gel aging time the samples were prepared to age for (4days) and crystallized for 8 hours at 110 ºC as the optimum crystallization condition for Zeolites synthesis (Ayele *et al.,* 2018)

Crystallization

The enclosed gel found in the autoclave reactor was then placed in the electric oven at 110 ºC for 8 hours for crystallization of Zeolite to take place, The reaction was then quenched with cold water to cease the crystallization process.. Olaremu *et al.,* (2018). The zeolite formed was washed thoroughly several times with deionized water, The pH was monitored, while washing, using Micro Processor pH- meter to obtain a pH of 8. The precipitated solid was filtered, air dried in the laboratory for 24hrs and finally dried in an oven at 100 ºC for 4 hours. The crystals were then pulverized for characterization.

Adsorption Experiments on Performance Test

The batch adsorption experiment was generally carried out using an adsorbent loading of 20 mg, at pH of 4-9 and at a room temperature of 25°C. During the experiment, 15 mL of 2 mg/L concentration of NH_3 solution was added to 20 mg of zeolite-based materials in a cuvette, and the absorbance was collected over a period of 2 hours. This procedure was repeated using 4, 8, and 12 hours interval study the effect of time on equilibrium (Al-Sheikh *et al*., 2020).

From the adsorption experiments, the adsorption capacity, *q*t (mg/g) equation (1), which represents the amount of dye adsorbed per unit weight of zeolite and the NH_3 removal efficiency, (*R*%) equation (2), were calculated as follows:

Adsorption capacity, qt = $\frac{(C_O-C_t)V}{W}$

Removal efficiency (%), R = $\frac{C_O-C_t}{C_O} \times 100$

Where C_0 is the ammonia concentration at time $t = 0$ (mg/L), Ct is the ammonia concentration at time $t = t$ (mg/L), V is the volume of ammonia solution (mL), and W is the mass of adsorbent used (mg). The absorbance was measured using UV-Vis spectrophotometer at the ammonia characteristic monochromatic wavelength (λ max) of 340 nm.

RESULTS AND DISCUSSION

Results of X-ray Fluorescence (XRF)

The results on Table 4.1 show that raw Oke-Ako kaolin contains contaminations of oxides of iron, titanium and Calcium, with increased value of these oxides listed, with the value of SiO_2 increased from 44.05% to 56.57% due to compensation of the whole proportion. The Table also show that Oke-Ako kaolin is ferric in nature due to its high content of iron oxide as compared with that of calcium oxide. It can also be observed that there is removal of Na_2O following the purification processes. Pure raw kaolin clay has a Silica/Alumina value of between1.5 to 3.5 (Ayele *et al.,* 2015, Ajayi *et al.,* 2010, Fentaw, 1998). The table 1 shows that the SiO_2/Al_2O_3 value of 3.21 and 2.97 for the raw and beneficiated kaolin respectively are within theoretical value (Villemiana *et al.*,2019) There was also a gradual decrease in the moisture content from the raw sample to the metakaolin sample, also an increased in the value of the loss in ignition (LOI) from raw sample to beneficiated sample which eventually dropped in metakaolin value sample.

XRF Analysis

The XRF data showed the expected high Si:Al value range of 1.90 to 1.95 for the alternative and 15.52 to 18.60 for the conventional methods respectively for zeolite-X synthesis from Oke-Ako samples stated in table 4.2. However, the results showed that a better ratio was achieved for both calcined sodium zeolite-X (ZNa-X) and dealuminated 5min sodium zeolite-X (D5ZNa-X) after treatments, compared to the raw Oke-Ako kaolin.

The result of X-ray diffraction (XRD) pattern for the raw Oke-Ako kaolin (OAK) analysis of the peaks show many sharp peaks, with low intensity at $2\theta = 12.34^o$. This is the main peak used in the identification of kaolinite clay (Ramirez, 2007). Also, the peak obtained at position corresponding to $2\theta = 27.90^o$ indicated the presence of large quantities of quartz. Kaolinite and quartz are predominant characteristics of natural kaolin (Tracy and Higgins, 2007, Ayele, L *et. al*., 2015). Hence, the high level of quartz in Oke-Ako kaolin is not surprising because it is in agreement and similar to Ayele *et al.*,(2015). The noticeable difference is in the values of the Loss on ignition (LOI) which increased from 7.66% to 8.83% for raw and beneficiated samples while there was a decrease in the metakaolin sample to 1.16% respectively this was due to the burning off of impurities such as Illite, orthoclase, osumilite e.t.c during calcination. As evident in Table 4.1, the compositional analysis of the beneficiated Oke-Ako kaolin indicates an increased in the composition of its free silica, alumina, titanium and other impurities using the conventional method of purification. It is expected that purification or beneficiation of raw Oke-Ako kaolin had shifted down its silica/alumina (SiO_2/Al_2O_3) value from 3.2 to 2.9. While the value of sodium oxide recorded 00.0 due to complete removal during beneficiation.

Table 1: XRF Compositional analysis results of the Raw, Beneficiated and Calcined Oke-Ako Kaolinite Oke-Ako Kaolinite (Wt. %)

OXIDES	Raw Oke-Ako Kaolinite	Beneficiated Oke Ako Kaolinite	Calcined Oke-Ako Kaolinite
SiO_2	44.05	56.57	43.26
Al_2O_3	23.33	32.34	41.39
Fe_2O_3	1.77	4.68	2.28
TiO_2	2.04	4.42	2.24
Na_2O	27.79	0.00	0.00
CaO	0.04	0.12	0.08
Total	99.02	98.13	89.25
Moisture content	1.38	0.14	0.05
L.O.I*	7.66	8.83	1.16
SiO_2/AlO_3 Value	**3.21**	**2.97**	**1.78**

Loss on ignition*

Metakaolinization of Oke-Ako kaolin

The XRF analysis of metakaolin presented in Table 4.1 shows that there were reduction in the oxides of Fe_2O_3, TiO_2 from 4.68 to 2.28 and 4.42 to 2.24 respectively in chemical composition of the calcined Oke-Ako kaolin due to organic components and impurities burnt out. The noticeable difference is in the values of Na_2O which decreased from 27.79 to 0.00 with a slight reduction in the SiO_2 / Al_2O_3 ratio from 2.97 to 1.78 for beneficiated and calcined samples respectively. As a result, the calcination of Oke-Ako kaolin from room temperature to $450^{o}C$ brings a loss in one of the sharp peaks as observed in Figure 4.6 due to the loss of the hydration water, which results in a better ordering in the structure of the kaolin molecules. However, there was complete loss of the main peaks reflection at $650^{o}C$ leaving only a small holes which indicate the formation of a non-crystalline phase. This is in good agreement with results of (Martinez *et al* 2013), which show the formation of metakaolin at a temperature around $650^{o}C$. The peaks at $2\theta = 12.34^{o}$ (kaolinite peak) disappeared but the peak at $2\theta = 26.67^{o}$ was not affected by the thermal treatment, attributed to the presence of quartz. Therefore, metakaolin can be described as an amorphous material containing free silica, free alumina as reported by (Edomwonyi-Otu *et al.,* 2013). The compositional silica /alumina ratio was reduced to 1.78 after calcination.

Dealumination of Metakaolin Sample

Dealumination is an alternative route to reduce the alumina content from the metakaolin, as a results it increases the $SiO_2:Al_2O_3$ values of the starting material. Adjusting the silica to alumina ratio was the key steps in the starting gel of high silica zeolite-X synthesis. Increased in the composition of its free silica, alumina, titanium and other impurities using the conventional method of dealumination, which was not similar to alternative method due to slight decrease in some of the parameters below. (Babalola *et al* 2015).

Table 2: X-ray fluorescence (XRF) compositional analysis of Dealuminated Oke-Ako Calcination using the Alternative and Conventional method by varying the time

Dealumination		Alternative Method (Time in minutes)			Conventional Method (Time in minutes)		
Oxide	**Calcined values**	**5**	**10**	**15**	**5**	**10**	**15**
SiO_2	43.26	43.61	43.11	45.59	46.82	84.06	85.94
Al_2O_3	41.39	38.02	38.53	40.58	40.96	9.21	7.85
Fe_2O_3	2.28	2.12	2.04	2.19	0.67	1.24	1.05
TiO_2	2.24	2.23	2.14	2.28	1.99	3.60	3.37
Na_2O	ND	ND	ND	ND	18.96	0.00	0.00
CaO	0.07	0.03	0.04	0.03	0.23	0.34	0.12
SiO_2/Al_2O_3	**1.78**	**1.95**	**1.90**	**1.90**	**1.95**	**15.52**	**18.60**

X-Ray Diffraction Analysis of D5ZNa-X and ZNa-X Zeolite-X

Powder X-ray diffraction was used to determine the sample crystallinity. The formation of zeolite-X from Oke-Ako kaolin was ascertained by comparing its XRD pattern of record to that of International Zeolite Association (IZA) powder pattern identification diffractograms, indicating a Faujasite structure (FAU). As illustrated by Treacy and Higgins within a range of $2\theta = 5\text{-}50^{\circ}$, the first peak for zeolite X will appear within 6-10˚. (Treacy *et al.,* 2001). The first three strongest peak for each zeolite (D5ZNa-X) was observed at $2\theta = 6.76^{o}$, 12.95^{o} and 24.95^{o} then $2\theta = 6.33^{\circ}$, 26.8^{o} and 31.2^{o}, for ZNa-X as both Zeolites have similar gel aging time of four day respectively. Small zigzag peaks refer to the presence of amorphous material. Strong peaks represent full crystallization. Also the SEM graphs represented by Plates 4.1a and 4.1b respectively have also confirmed the successful synthesis of zeolite-X. Synthesized zeolite-X gave similar FT-IR spectrum and SEM morphology patterns (Kovo *et al.,* 2012; Ekpe *et al.,* 2017).

Table 3: XRD results of the BOK, COK, D5ZNa-X and ZNa-X

Sample	Kaolinite Peak positions	Quartz Peak positions
BOA	12.34^{o} (14%)(Ramirez, 2007).	27.90^{o} (55%)Ayele, *et. al.*, 2015
COA	Nil	26.67^{o} (Edomwonyi-Otu, *et al.*, 2013).
D5 ZNa-X	$2\theta = 6.76^{o}$, 12.95^{o} and 24.95^{o}	20.10^{o}, 27.00^{o}and 68.01^{o}
ZNa-X	$2\theta = 6.33^{o}$,26.8^{o} and 31.2^{o},	27.50^{o}, 60.2^{o}, and 60.9^{o}

(Kovo *et al.*, 2012 ; Ekpe *et al.*, 2017)

Figure 1 is showing the superimposed of the two synthesized Zeolites D5ZNa-X and ZNa-X, subtend at the 2θ (Theta) Braggs angles 6.33^{0}, 26.80^{0}, 31.20^{0} for ZNa-X and the Braggs angles for D5ZNa-X were 6.76^{0}, 12.95^{0} and 24.95^{0}respectively. However, the Quartz subtends at the 2θ (Theta) Braggs angles of 20.10^{0}, 27.20^{0},60.90^{0} for ZNa-X and the quartz for D5ZNa-X subtends at the 2θ (Theta) Braggs angles of 20.10, 27.00^{0} and 68.01^{0} respectively. Therefore showed sharp peaks, indicating that both samples were crystalline at this stage. The patterns matched with both synthetic and commercial Na-X zeolite XRD patterns as reported by (Bai *et al.*, 2018). It was also similar to the (not de-aluminated) untreated metakaolin reported by (Konne *et al.*, 2016). The sharper peaks and lower broad background on the XRD pattern of Oke-Ako indicated that the D5ZNa-X was more crystalline while the untreated calcined ZNa-X has a larger surface area value, which were the main characteristics of zeolite.

Table 4: Revealed the summary of percentage minerals in D5ZNa-X sample

Mineralogy of D5ZNa-X	Percentage
Zeolites	30.5%
Quartz	51.6%
Nitrolite	0.8%
Mordenite	0.7%

Table 5: Revealed the percentage mineral content of ZNa-X sample

Mineralogy of ZNa-X sample	Percentage (%)
Zeolites	25%
Quartz	50%
Mordenite	0.8%
Nitrolite	0.5%

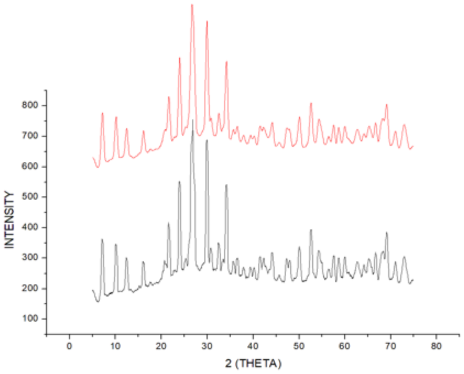

Figure 1: Showing the XRD pattern of superimposed ZNa-X and D5ZNa-X

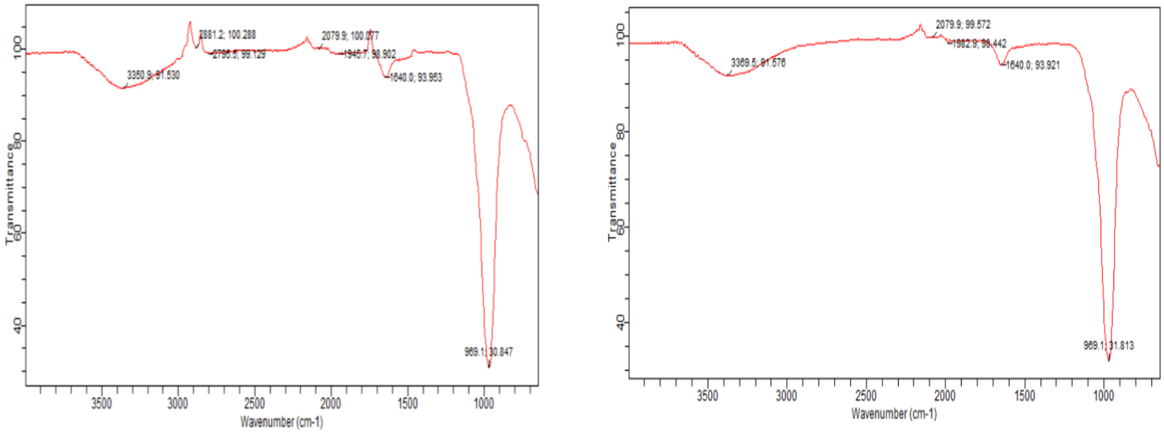

FT-IR spectra of zeolite D5ZNa-X sample

FT-IR spectra of zeolite ZNa-X sample

Figure 2: FT-IR spectra of D5ZNa-X and ZNa-X samples from Oke-Ako kaolin

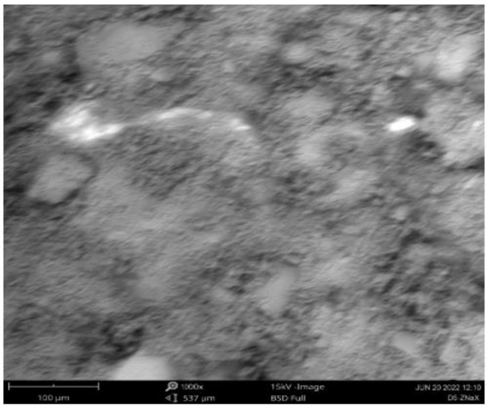

Plate 1a: SEM Image of D5ZNa-X at x100µm

Plate 1b: SEM Image of ZNa-X at x100µm

FT-IR (Fourier Transformed Infra-red)

FT-IR Analysis

Fourier Transformed Infra-Red analysis was carried out on BOA, COA, D5ZNa-X and ZNa-X. The characterization was carried out between 650 and 4000 cm $^{-1}$. Strong bands at 3690, 3652, 3452 cm^{-1} were observed for the beneficiated sample. No prominent peak was observed between 3000 and 1100 cm^{-1} except at 2083 for calcined sample. A number of peaks with variable intensities were observed in the range of 1200 cm^{-1} – 800 cm^{-1} region for the beneficiated sample.

However, the transmittance intensity was reduced in the calcined sample (from 10% to 45%) and the peaks even out in the COA, in the same vein the calcination resulted in loss of OH peaks which were present in the beneficiated sample at 3690 cm^{-1} This could be associated with increased in porosity due to metakaolinization. Therefore, strong peaks (low transmittance) at 3450cm^{-1} (OH region) indicates the zeolites has an abundance of hydroxyl group (Adeyanju *et al*., 2016, Lu *et al.,* 2019). in ZNa-X and D5ZNa-X respectively. The higher intensity of the D5ZNa-X peaks above the ZNa-X agreed with the XRD and SEM of higher crystallinity of D5ZNa-X over ZNa-X. (Pandianga, K *et al.,* 2017).

Table 6: Revealed the FT-IR summary Data cm^{-1} range of all the Samples

Assignments	BOK	COK	D5ZNa-X	ZNaX	Literature	Reference
OH *Stretch Vibration*	3690	—	—	—	3694	(Rios. *et al*.,2008)
OH *absorbed* ***H₂O*** *molecule*	—	—	3362	3362	3447	(Weia. *et al.*,2015)
H₂O *adsorption Band*	—	—	1651	1640	1645	(Pandianga. *et al.,* 2017)
C=C *bond in aromatic comps*	—	—	1394	—	1430	(Taju, 2016)
Si-O-Si *Stretching*	988	—	969	969	1005	(Elizabeth, 2016)
Symmetric ***Si-O-Si*** *Stretching*	790	790	—	—	797	(Aniela, 2017)
Asymmetric ***Si-O-Si*** *Stretching*	1114	1058	—	—	1035	(Aniela, 2017)

FT-IR spectroscopy in Table 6 was used to probe the structures of D5ZNa-x and ZNa-X and to monitor reactions in zeolite pores. The FT-IR spectrum bands at 3690 Cm^{-1} Beneficiated Oke Ako kaolin (BOA) correspond to the OH stretching vibrations on the surface of kaolinite (Rios .A.*et al*.,2008). A critical examination of the results revealed some major changes in the spectra of the samples. These are:

A shift in the wave number of adsorption from a lower wave number to a higher wave number was observed (hyperchromic effect). In this case, the intensity of the adsorption band was found to increase in D5ZNa-X. (Ameh *et al.,* 2015).

Disappearance and appearance of some adsorption band of the samples for BOA and COA is as a result of calcination on ZNa-X while D5ZNa-X is as a result of dealumination. The extent of the frequency shift can be directly attributed with the high level of specific molecular interactions such as hydrogen and dipole-dipole interactions. From the results obtained, hypochromic shifts were observed for C-N stretch and C=C stretch. Those functional groups, missing might have been used for the formation of new bands. (El-Yukub *et al.,* 2020).

Analysis of Brunauer-Emmett-Teller (BET)

The Table 5 above shows BET results of calcined and dealuminated samples of Zeolites. D5ZNa-X had a lower specific surface area value of 145.85 m^2/g and pore volume of 0.090 cc/g. The surface area of D5ZNa-X decreased by 151% on dealumination for 5minutes while the pore volume decreased exponentially by 30%. The decreased in the surface area may be attributed to dealumination process of the kaolin mineral to the highly amorphous metakaolin as shown by the XRD patterns of the materials. The ordered platelets structure of kaolinite as a result of calcination as shown by SEM images had resulted into highly surface area in ZNa-X than the dealuminated D5ZNa-X sample. (Bansiwal *et al.,* 2010).

Table 7: Revealed the Colour, BET summary analysis of the (neat) parent Zeolites and the encapsulated metal catalyst complexes

Catalysts	Colours	BET Surface area m^2/g	Pore volume cc/g
ZNa-X	Light brown	323.62	0.165
D5ZNa-X	Dark brown	145.85	0.131

Impact of pH on the percentage removal of ammonia using four different prepared zeolite-based adsorbents

The impact of pH values on NH_3 adsorption by using the prepared zeolites adsorbents were performed by adjusting pH values in a range from 4.0 to 9.0 as shown in Table 8 depicts the adsorption capacities of the four different ziolite-based adsorbent. The results indicate a clear pH-dependent behavior in ammonia adsorption capacity using ZNa – X (Calcined neat Zeolite sample).

Table 8: Removal of ammonia by ZNa – X Calcined sample

C_o(mg/L)	pH	%ABSORBANCE	C_t (mg/L)	% Removal	Adsorption capacity (mg/g)
15	4	0.268	0.692	95.39	10.73
15	5	0.180	0.465	96.90	10.90
15	6	0.211	0.545	96.37	10.84
15	7	0.313	0.808	94.61	10.64
15	8	0.264	0.681	95.46	10.74
15	9	0.206	0.532	96.45	10.85

At pH 4, the adsorption capacity was found to be 10.73 mg/g. The highest adsorption capacity of 10.90 mg/g was achieved at pH 5. However, beyond pH 5, a slight decrease in adsorption capacity was observed. The adsorption capacity at pH 6 was found to be 10.84 mg/g. The adsorption capacity generally increased as the pH level shifted from acidic (pH 4) to neutral (pH 7). This trend can be attributed to the increasing presence of uncharged ammonia (NH_3) molecules at lower pH, which can readily interact with zeolite surfaces . However, the adsorption capacity increases at pH levels of 8 and 9 with the values of 10.74 and 10.85 mg/g respectively. This may be due to the abundance of hydroxide ions (OH^-) in the solution which may compete with ammonia for adsorption sites, leading to a reduction in adsorption capacity (Lina *et al.*, 2013). At lower pH values (acidic conditions), ammonia exists predominantly as uncharged NH_3 molecules, which are more easily adsorbed.

Table 9: Removal of ammonia by D5 – ZNa – X (Dealuminated) sample

C_o(mg/L)	pH	%ABSORBANCE	C_t (mg/L)	%Removal= $\frac{C_O-C_t}{C_O}\times 100$	A. capacity, qt = $\frac{(C_O-C_t)V}{W}$
15	4	0.071	0.185	98.77	11.11
15	5	0.032	0.084	99.44	11.19
15	6	0.188	0.486	96.76	10.89
15	7	0.062	0.162	98.92	11.13
15	8	0.120	0.311	97.93	11.02
15	9	0.008	0.023	99.85	11.23

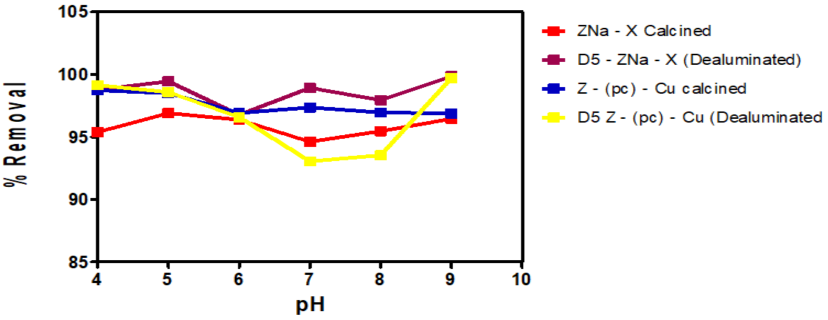

Figure 3: Impact of pH on NH_3 removal efficiency from liquid by four different adsorbent.

For D5 – ZNa–X (Dealuminated neat Zeolite sample**),** the results proved that the adsorption process in the current study was somewhat pH-dependent. The adsorption capacity of ammonia was highest at pH 9 with a value of 11.23 mg/g while the lowest was found at pH 6 with a value of 10.89 mg/g. The present study observed the same trend in a pH rise with other literatures **(**Safie *et al.*, 2019**).**

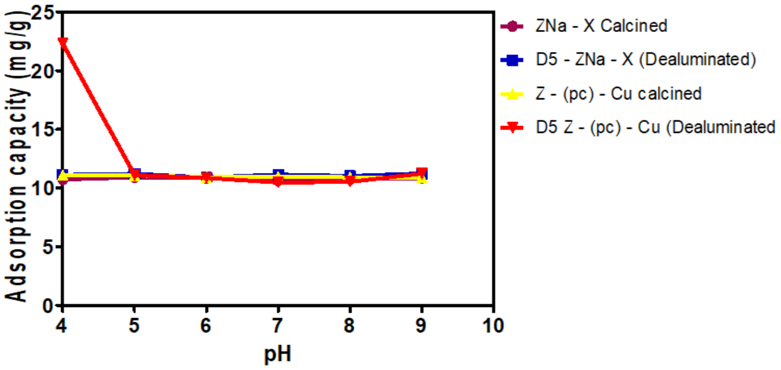

Figure 4: Impact of pH on NH_3 adsorption capacity by four different adsorbent

Impact of time on the percentage removal of ammonia using four different prepared zeolite-based adsorbents

At the 2-hour mark, the adsorption capacity is 12.21 mg/g. This represents the initial rapid adsorption phase, where ZNa - X Calcined quickly capture ammonia from the solution due to available adsorption sites. As time progresses to 4 hours, the adsorption capacity increases to 12.46 mg/g. This indicates that ammonia adsorption onto adsorbents continues to occur, albeit at a slightly reduced rate compared to the initial phase. By the 8-hour mark, the adsorption capacity reaches 13.36 mg/g. This suggests that ammonia adsorption is approaching equilibrium, where the rate of adsorption becomes nearly equal to the rate of desorption. At this point, further increases in adsorption capacity are minimal. Finally, at the 12-hour mark, the adsorption capacity stabilizes at 15.45 mg/g. This value represents the maximum ammonia adsorption capacity achievable under the given conditions and highlights that ZNa-X Calcined have effectively captured ammonia from the solution. Similar findings was observed for D5 - ZNa - X (Dealuminated); 12.64mg/g at 2-hour mark, 12.78mg/g at 4-hour mark, 13.67mg/g at 8-hour mark and 14.34mg/g at 12-hour mark, Z - (pc) - Cu calcined catalyst; 11.98mg/g at 2-hour mark, 12.62mg/g at 4-hour mark, 13.20mg/g at 8-hour mark and 14.20mg/g at 12-hour mark, and D5 Z - (pc) - Cu (Dealuminated; 13.01 mg/g at 2-hour mark, 14.70mg/g at 4-hour mark, 14.90 mg/g at 8-hour mark and 15.40 mg/g at 12-hour mark. The results are presented in Figure 4.14. Generally, the graphs show that the amount of NH_3 molecules adsorbed increased with contact time for all the adsorbents.

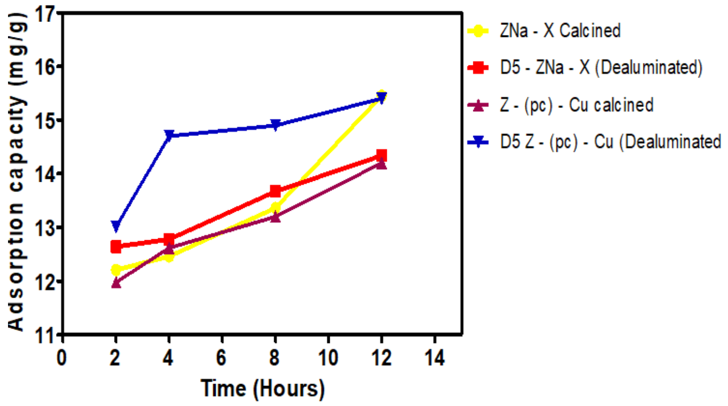

Figure 5: Impact of time on NH_3 adsorption capacity by four different adsorbent

Effect of pH on the percentage removal of ammonia using four different prepared zeolite-based adsorbents

The impact of pH values on NH_3 adsorption by using the prepared adsorbents were performed by adjusting pH values in a range from 4.0 to 9.0 as shown in Figure 3, among the initial pH values, the maximum ammonium adsorption takes place at pH 5.0 with the value of 96.90%. The percentage removal increased as the pH level shifted from acidic (pH 4) to (pH 6). The values are found to be 95.39, 96.90 and 96.37% at pH 4, 5 and 6 respectively. This trend is consistent with the increased presence of ammonia (NH_3) molecules at lower pH levels, which are more easily adsorbed by ZNa–X Calcined. The increase in ammonia removal at increased pH and initial ammonia concentration suggests the interplay of molecular adsorption mechanism (Weia *et al*., 2015).

Impact of time on the percentage removal of ammonia using four different prepared zeolite-based adsorbents

At the 2-hour mark, the percentage removal of ammonia is 94.20%. During this early stage, a substantial portion of ammonia has been adsorbed by the ZNa - X Calcined, but the removal process is ongoing. As time progresses to 4 hours, the percentage removal increases to 96.50%. This indicates that the ammonia removal process continues to improve with time, with more ammonia molecules being captured by the zeolite adsorbents. By the 8-hour mark, the percentage removal reaches 97.40%. This suggests that the ammonia removal process is approached optimal efficiency, with a significant portion of ammonia removed from the solution (Nyankson *et al*., 2019). This value represents the maximum ammonia removal efficiency achievable under the given conditions (Sanchez-Hernandez *et al*., 2018). Finally, at the 12-hour mark, the percentage removal reduced to 93.30%.

Table 10: Effect of time on % removal of ammonia by the samples

Time (hours)	ZNa - X Calcined	D5 - ZNa - X (Dealuminated)
2.00	94.20	92.43
4.00	96.50	94.53
8.00	97.40	97.90
12.00	93.30	95.50

Table 11: Effect of time on adsorption capacity by the samples

Time (hours)	ZNa - X Calcined	D5 - ZNa - X (Dealuminated)
2.00	12.21	12.64
4.00	12.46	12.78
8.00	13.36	13.67
12.00	15.45	14.34

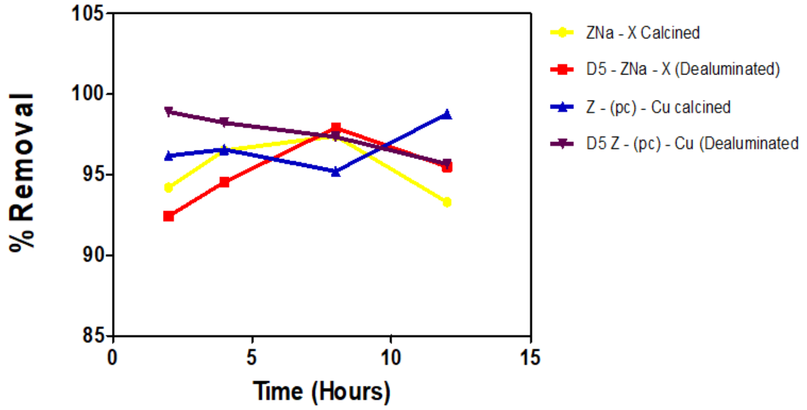

Figure 6: Impact of time on the removal of NH_3 by the adsorbents.

CONCLUSION

Zeolite-X was successfully synthesized from clay sourced from Oke-Ako of Ijebu-Ode, Ogun state, Nigeria after alkaline treatment of its metakaolin which depended solely on the ageing time, reaction temperature, metakaolinization temperature and NaOH concentration. The X-ray fluorescence (XRF), X-ray diffraction (XRD) analysis confirmed the presence of zeolitic mineral phases in both D5ZNa-X and ZNa-X crystallized samples respectively. However, the D5ZNa-X sample was more crystalline as shown by sharper intense XRD peaks, rougher surface on the SEM micrograph and sharper bands on the FT-IR. Both samples had similar bands especially the characteristic zeolitic O-H stretching at 3362Cm^{-1} and Si-O Stretching at 969 cm^{-1}. and also showed the absence of some toxic metals implying that the synthesized zeolites were safe and environmentally friendly. According to this study's results, the dealumination process was optional since, zeolite-X was synthesized successfully with or without the dealumination process, except in their percentage of crystalinity, as D5ZNa-X is more crystalline than ZNa-X. These results also illustrate the intricate interplay of different parameters on ammonia adsorption capacity using zeolites. Dose-dependent, pH-dependent and time-dependent trends were observed, providing valuable insights into the behaviour of zeolite adsorbents in ammonia removal processes and developing efficient, sustainable environmental remediation solution. A lot of work has been done in this area and has successfully produced high quality synthesized zeolites like zeolite A, X and Y from Nigerian kaolin. However, zeolite-X synthesis from novel Oke-Ako will have a greater role as a catalyst in adsorption of small molecules. Using natural raw material like Kaolin will cut down cost considerably as local materials are cheaper than purchasing chemicals.

REFERENCES

Adeyanju, O., Olademehin, O. P., Nwanta, U. C., Adejoh, A. I., Hussaini, Y., & Plavec, J.(2016).Synthesis and characterization of carboxymethyl Plectranthus esculentus starch. A potential disintegrant. Journal of Pharmaceutical and Applied Chemistry, 2(3), 44-50.

Ameh P.O Kohapu and Eddy N.O (2015). Experimental and quantum chemical studies on the corrosion inhibition potential of phthalic acid for mild steel in 0.1M H_2SO_4 chemical Sciences Journal 6:3.

Aniela Z. (2017). Chemical modifications of hollow silica microspheres for the removal of organic pollutants in simulated wastewater. [Dissertation] Abdullah University of science and technology, Saudi Arabia; 201-207. anthelmintic carriers. J Helminthol. 2000; pp. 74: 137– 141.

Al-Sheikh, F., Moralejo, C., Pritzker, M., Anderson, W. A., & Elkamel, A. (2020). Ammonia removal from real wastewater using a LEWATIT S 108 H resin: A batch process and fixedbed column. Separation Science and Technolog

Ayele, L. (2018). Synthesis of zeolite A using raw kaolin from Ethiopia and its application in removal of Cr (III) from tannery wastewater. Journal of Chemical Technology & Biotechnology. 93(1): 146-154.

Ayele, L., *et al*, (2016). Conventional versus alkali fusion synthesis of zeolite A from low grade kaolin. Applied Clay Science. 132-133: 485-490.

Babalola, R., et al, (2015). Comparative Analysis of Zeolite Y from Nigerian Clay and Standard Grade.

Bai, H.-X., Zhou, L.-M., Chang, Z.-B., Zhang, C. and Chu, M. (2018) Synthesis of Na- X Zeolite from Longkou Oil Shale Ash by Alkaline Fusion Hydrothermal Method. Carbon Resources Conversion, 1, 245-250. https://doi.org/10.1016/j.crcon.2018.08.005

Bansiwal A, Pillewan P, Biniwale R.B and Rayalu A.S (2010) Copper incorporated mesoporous Alumina for defluoridation of drinking water, microporous and mesoporous, 129:54-61

Edomwonyi-otu, L. C., Aderemi, B. O., Ahmed, A. S., Coville, N. J., &Maaza, M. (2013). Influence of Thermal Treatment on Kankara Kaolinite. Optican 1826, 15(5), 1–5.http://doi.org/http://dx.doi.org/10.5334/opt.bc

Elizabeth V. (2016). Synthesis and characterization of zeolites from bauxite and kaolin: application to the removal of heavy metals from mining wastewater. [Dissertation] Kabwe: Kwame Nkrumah University, Zambia;

El-Yaqub and S.O Okeniyi (2020) Corrosion studies of Aluminium alloy in 0.1M H_2SO_4 by extracts of balanitesaegyptiaca Science view Journal (SCVJ) volume 1no 2 81-87.

Ekpe, I., (2017). Zeolite Synthesis, Characterization and Application Areas: A Review. Vol. 6.

Emmanuel Nyankson, Jonas Adjasoo, Johnson Kwame Efavi , Reuben Amedalor, Abu Yaya, Gloria Pokuaa Manu, Kingsford Asare, and Nii Amarkai Amartey (2019). Characterization and Evaluation of Zeolite A/Fe3O4 Nanocomposite as a Potential Adsorbent for Removal of Organic Molecules from Wastewater. Hindawi Journal of Chemistry Volume, Article ID 8090756, 13 pages https://doi.org/10.1155/2019/8090756

He, Y., Tang, S., Yin, S., & Li, S. (2021). Research progress on green synthesis of various high-purity zeolites from natural material-kaolin. *Journal of Cleaner Production*, *306*, 127248.

Kovo, A.S.(2012). Effect of Temperature on The Synthesis of Zeolite X from Ahoko Nigerian Kaolin Using Novel Metakaolinization Technique. Journal of Chemical Engineering Communications, Volume 199, - Issue 6 786-797. http://dx.doi.org/10.1080/ 00986445.2011.625065.

Maciver, V. P., Dagde, K. K., & Konne, J. L. (2020). Synthesis of zeolite X from locally sourced kaolin clay from Kono-Boue and Chokocho, Rivers state, Nigeria. Advances in Chemical Engineering and Science, 10(4), 399-407.

Noviello, M., Gattullo, C. E., Faccia, M., Paradiso, V. M., & Gambacorta, G. (2021). Application of natural and synthetic zeolites in the oenological field. *Food Research International*, *150*, 110737.

Olaremu, A., Odebunmi, E. and Nwosu, F. (2018) Synthesis of Zeolite from Kaolin Clay from Erusu South western Nigeria. Journal of Chemistry Society of Nigeria, 43, 381-786.

Rios A, Williams D, Roberts L. (2008). Removal of heavy metals from acid mine drainage using coal fly ash, natural clinker and synthetic zeolites. :156(1-3):23–35, 20 : https://doi.org/10.1016/j.jhazmat.2007.11.123

Ruth Sa´nchez-Herna´ndez ,1 Isabel Padilla ,1 Sol Lo´pez-Andre´s ,2 and Aurora Lo´pez-Delgado (2018). Al-Waste-Based Zeolite Adsorbent Used for the Removal of Ammonium from Aqueous Solutions. Hindawi. International Journal of Chemical Engineering Volume 2018, Article ID 1256197, 11 pages https://doi.org/10.1155/2018/1256197.

Taju S. (2016). Synthesis of nano hydroxyapatite/ stilbite composite for defluoridation of drinking water. [dissertation] Addis Ababa University, Ethiopia.

Treacy, M. M. J., & Higgins, J. B. (2001). Collection of simulated XRD powder patterns for zeolites. (5th ed.). Elsevier B.V. http://doi.org/10.1016/S0166-9834(00)81382-2.

Pandiangan K, Arief S, Jamarun N, Simanjuntak W. J Mater Environ Sci (2017). Synthesis of Zeolite-X from Rice Husk silica and aluminum metal as a catalyst for transesterification of palm oil. 8(5):1797–1802.

Pérez-Botella, E., Valencia, S., & Rey, F. (2022). Zeolites in adsorption processes: State of the art and future prospects. *Chemical Reviews*, *122*(24), 17647-17695.

Vera-Puerto, I., Saravia, M., Olave, J., Arias, C., Alarcon, E., & Valdes, H. (2020). Potential application of chilean natural zeolite as a support medium in treatment wetlands for removing ammonium and phosphate from wastewater. *Water*, *12*(4), 1156.

Weia G, Yanga L, Zhonga W, Li S. (2015). Fast removal of methylene blue from aqueous solution by adsorption onto poorly crystalline hydroxyapatite nanoparticles. J NanomaterBiostruct;10(4):1343–1363.